Brain anatomical networks in world class gymnasts: A DTI tractography study

Bin Wang [a], Yuanyuan Fan [a], Min Lu [b,c], Shumei Li [a], Zheng Song [b], Xiaoling Peng [a], Ruibin Zhang [a], Qixiang Lin [b], Yong He [b], Jun Wang [b,*], Ruiwang Huang [a,**]

[a] Center for the Study of Applied Psychology, Key Laboratory of Mental Health and Cognitive Science of Guangdong Province, South China Normal University, Guangzhou 510631, PR China
[b] State Key Laboratory of Cognitive Neuroscience and Learning, Beijing Normal University, Beijing 100875, PR China
[c] Institute of Psychology, Chinese Academy of Sciences, Beijing 100101, PR China

ARTICLE INFO

ABSTRACT

The excellent motor skills of world class gymnasts amaze everyone. People marvel at the way they precisely control their movements and wonder how the brain structure and function of these elite athletes differ from those of non-athletes. In this study, we acquired diffusion images from thirteen world class gymnasts and fourteen matched controls, constructed their anatomical networks, and calculated the topological properties of each network based on graph theory. From a connectivity-based analysis, we found that most of the edges with increased connection density in the champions were linked to brain regions that are located in the sensorimotor, attentional, and default-mode systems. From graph-based metrics, we detected significantly greater global and local efficiency but shorter characteristic path length in the anatomical networks of the champions compared with the controls. Moreover, in the champions we found a significantly higher nodal degree and greater regional efficiency in several brain regions that correspond to motor and attention functions. These included the left precentral gyrus, left postcentral gyrus, right anterior cingulate gyrus and temporal lobes. In addition, we revealed an increase in the mean fractional anisotropy of the corticospinal tract in the champions, possibly in response to long-term gymnastic training. Our study indicates that neuroanatomical adaptations and plastic changes occur in gymnasts' brain anatomical networks either in response to long-term intensive gymnastic training or as an innate predisposition or both. Our findings may help to explain gymnastic skills at the highest levels of performance and aid in understanding the neural mechanisms that distinguish expert gymnasts from novices.

Introduction

A major challenge for modern neuroscience is to uncover the plastic changes that occur in human brain structure when people participate in intensive motor training (Draganski et al., 2004), learn a new skill (Mechelli et al., 2004; Schmithorst and Wilke, 2002), or adapt to a neuropathology (Keller and Just, 2009; Oh et al., 2009). Structural plasticity is an intrinsic property of the human brain and enables people to achieve their best behavioral performance under a variety of conditions (Pascual-Leone et al., 2005).

Previous studies, applying cross-sectional or longitudinal study designs, have showed that motor skill acquisition and training can induce changes in the structural properties of specific brain areas that are involved in a practiced task. Recent longitudinal neuroimaging studies have focused on the effects of motor training lasting several days or weeks in previously untrained subjects and have showed plastic changes in specific white matter (WM) regions (Scholz et al., 2009; Taubert et al., 2010). However, longitudinal studies investigating training-induced changes in anatomical properties of the brain are time consuming and often nearly impossible if the training occurs over long time periods. Therefore, to examine practice-induced changes, such as brain structural differences in the relevant white matter, as induced by professional musical training (Bengtsson et al., 2005; Imfeld et al., 2009; Schmithorst and Wilke, 2002) and golf training (Jancke et al., 2009), most studies adopted a cross-sectional paradigm in which highly skilled subjects were compared with less-skilled subjects. However, the development of motor skills depends not only on the differential involvement of sets of relevant WM tracts but also on changes in the topologically structural connectivity patterns of the WM, as reflected by brain anatomical networks.

The development of neuroimaging techniques and graph theory has provided a new avenue of research for elucidating the large-scale topological organization of the human brain. Diffusion-weighted magnetic resonance imaging (DW-MRI) is the only available noninvasive technique for detecting WM fiber bundles in the human brain in vivo. Since Hagmann et al. (2007) first used DW-MRI and tractography to study human brain anatomical networks, whole-brain anatomical network investigations have been increasingly applied to explore the

* Corresponding author. Fax: +86 10 5880 2060.
** Correspondence to: R. Huang, Centre for Studies of Psychological Application, Key Laboratory of Mental Health and Cognitive Science of Guangdong Province, South China Normal University, Guangzhou 510631, PR China. Fax: +86 208521 6499.
E-mail addresses: jun_wang@bnu.edu.cn (J. Wang), ruiwang.huang@gmail.com (R. Huang).

changes in the brain anatomical networks that result from normal development and aging (Gong et al., 2009b; Yap et al., 2011) as well as those occurring in various diseases, such as Alzheimer's disease (Lo et al., 2010), multiple sclerosis (Shu et al., 2011) and schizophrenia (Zalesky et al., 2011). Descriptions of human brain anatomical networks have become especially attractive as they offer the possibility for more complete detection of specific neural systems. However, no study to date has compared the brain anatomical networks of elite athletes with those of non-athletes, specifically in world class gymnasts.

Gymnastics is a competitive sport that requires precise motor control, balance, power and focused attention during the execution of the motions. World class gymnasts are typical elite athletes in that a child will never grow into a world class gymnast without extensive training from a very young age and without practicing several hours a day so that they can achieve the excellent balance, strength and flexibility that will enable them to excel in competition. Therefore, changes in brain structure and anatomical networks may be expected to occur after long-term intensive gymnastic training. Thus, we expected to find differences between the topological properties of the anatomical network of gymnastic champions and those of controls in the motor-, visuospatial-, and attention-related brain regions.

Our goal was to investigate the characteristics of the world class gymnasts' brain anatomical networks using a cross-sectional approach. Therefore, we acquired diffusion tensor imaging (DTI) data from thirteen World-Cup or Olympic gymnastics champions and fourteen normal controls, constructed the anatomical networks for both subject groups using deterministic tractography, calculated the topological properties of the networks using graph theory, and performed statistical comparisons to pinpoint the differences in the anatomical networks between these two subject groups.

Materials and methods

Subjects

Thirteen world class gymnasts (M/F 6/7, aged 17–26 year, mean ± std = 20.5 ± 3.2 years) were recruited for this study. Each of them had trained for more than 10 years and attended gymnastic training at least 6 h per day. Table 1 shows the discipline, main demographics, number of years of training and the age of commencement for each gymnast. Each had won at least one gold medal in the Gymnastic World-Cup or Olympic Games (Table 1). We also recruited fourteen healthy age- and gender-matched undergraduates/graduate students (M/F 7/7, aged 19–28 years, mean ± std = 22.3 ± 2.7 years) as the controls. The age analysis was performed using a two-tailed two-sample t-test ($p = 0.10$). The gender data were analyzed using a χ^2 test ($\chi^2(1) = 0.04$, $p = 0.84$). All subjects were right-handed and had no history of neurological or

psychiatric disease or head injury. The protocol was approved by the Research Ethics Committee of the Institute of Cognitive Neuroscience and Learning at Beijing Normal University. Written consent was obtained from each participant prior to the magnetic resonance (MR) scanning.

Image acquisition

MR images were obtained using a Siemens Trio Tim 3 T MR scanner. Both DTI and 3D high resolution brain structural images were acquired using a 12-channel phased-array head coil with the implementation of the parallel imaging scheme GRAPPA (GeneRalized Autocalibrating Partially Parallel Acquisitions) and an acceleration factor of 2.

DTI data were acquired using a single-shot twice-refocused spin-echo diffusion echo planar imaging (EPI) sequence. The sequence parameters were repetition time (TR) = 10,000 ms, echo time (TE) = 92 ms, 64 non-linear diffusion directions with $b = 1000$ s/mm^2 and an additional volume with $b = 0$ s/mm^2, data matrix = 128 × 124, field of view (FOV) = 256 mm × 248 mm, 2 mm slice thickness, isotropic voxel size (2 mm)^3, bandwidth (BW) = 1502 Hz/pixel, and 75 transverse slices without gap covering the whole brain. The acquisition time was approximately 12 min for each DTI scan. Three DTI scans were acquired and were subsequently averaged in order to increase the signal-to-noise ratio (SNR).

We also acquired 3D high resolution brain structural images (voxel size = 1 mm^3, isotropic) using a T1-weighted MP-RAGE sequence for each subject. The sequence parameters were TR/TE = 1900 ms/ 3.44 ms, inversion time (TI) = 900 ms, flip angle = 9°, FOV = 256 mm × 256 mm, slice thickness = 1 mm, and 176 sagittal slices covering the whole brain. All subjects were scanned using the same MR scanner. For each subject, both the DTI data and the brain structural images were acquired in the same session.

DTI data preprocessing

For each subject, the three DTI datasets were concatenated into a 65 × 3 volumes dataset. The effects of head motion and image distortions caused by eddy currents were corrected by applying the affine alignment of all other diffusion-weighted images (65 × 3 volumes) to the first $b = 0$ volume in the original DTI measurement using the FSL-FDT Toolbox (Version 4.1; http://www.fmrib.ox.ac.uk/fsl). The corrected DTI dataset was split into three DTI datasets which corresponded to the three original DTI scans, respectively, but contained the modified values. The three corrected DTI datasets were then averaged to generate the averaged DTI data of 65 volumes.

Table 1
Characteristics of the world class gymnasts who participated in this study.

Champions	Discipline	Best medal records since 2007	Gender	Age (years)	Age of commencement (years)	Years of training (years)
1	Pommel horse	OC	M	24	4.5	19.5
2	Still rings	WC	M	24	4.5	19.5
3	Parallel bars	WC	M	23	4.5	18.5
4	Horizontal bar, AA	WC	M	26	4.5	21.5
5	Vault	OC	F	21	4.5	16.5
6	Uneven bars, AA	WC	F	17	4.5	12.5
7	Uneven bars, AA	OC	F	18	3.5	14.5
8	Floor exercises	OC	F	17	4.5	12.5
9	Uneven bars, AA	OC	F	17	4.5	12.5
10	Parallel bars, AA	WC	M	21	4.5	16.5
11	Uneven bars, AA	WC	F	19	4.5	14.5
12	Pommel horse	WC	M	23	4.5	18.5
13	Balance beam, AA	OC	F	17	4.5	12.5
Mean ± std				20.5 ± 3.3	4.4 ± 0.3	16.1 ± 3.3

Note: all of them have won individual or team gold medals in the Gymnastic World Championships or the Olympic Games since 2007 (OC = Olympic Champions, WC = World Champions or World-Cup Champions). The second column represents the dominant discipline for each of the champion subjects. AA: all around.

Network construction

We used the automated anatomical labeling (AAL) template (Tzourio-Mazoyer et al., 2002) containing 90 brain regions (see Inline Supplementary Table S1) to construct the human brain anatomical networks for each subject. Each brain region was defined as a node with each detectable anatomical connection between each pair of nodes as an edge. We estimated the topological properties of the human brain anatomical networks using graph theory. The procedure for constructing the brain anatomical networks can be found in previous publications (Gong et al., 2009a; Yan et al., 2011) (see Supplementary Materials Fig. S1).

Inline Supplementary Table S1 can be found online at http://dx.doi.org/10.1016/j.neuroimage.2012.10.007.

In brief, for each subject, we first coregistered the 3D brain structural images into the $b=0$ images using a linear transformation (Collignon et al., 1995). The resultant structural images in the diffusion space were then mapped to the T1 template of ICBM152 in the Montreal Neurological Institute (MNI) space using a nonlinear transformation. An inverse transformation was used to warp the AAL template from the MNI space to the diffusion space by a nearest-neighbor interpolation method. The linear and nonlinear transformations were all performed using the SPM8 package (http://www.fil.ion.ucl.ac.uk/spm/software/spm8). Next, we reconstructed the fibers linking each pair of brain regions in the diffusion space. The fibers for the whole brain were constructed using DTIstudio software (Version 3.0.3) based on the Fiber Assignment by Continuous Tracking (FACT) algorithm (Jiang et al., 2006). Fiber tracking was stopped at voxels where FA<0.2 and the angle between two eigenvectors of two consecutive voxels to be connected by the tracking was larger than 45°. The inter-regional connection density, which was obtained using fiber tractography, can be defined as the sum of the inverse of the fiber length between two nodes normalized by their mean volume (Hagmann et al., 2008)

$$w_{ij} = \frac{2}{s_i + s_j} \sum_{f \in F_e} \frac{1}{l(f)},$$

where s_i and s_j stand for the cortical surfaces area of brain regions i and j that were connected via an edge $e(i,j)$, F_e stands for the all fibers connecting regions i and j, and $l(f)$ stands for the length of the fiber f. In order to retain more information and to reflect the heterogeneity in the capacity and intensity of the connections, we used the unthresholded inter-regional connection density to define the edge. In this way, we obtained a symmetrical anatomical 90×90 matrix and a weighted anatomical network for each subject.

Network analysis

Global parameters of the human brain anatomical networks

The topological properties of human brain anatomical networks can be analyzed quantitatively using graph theory (Bullmore and Sporns, 2009; Hagmann et al., 2010). The global properties of a graph $G(N, M)$ with N nodes and M edges can be characterized by the following parameters: weighted clustering coefficient (C_w), characteristic path length (L_w), global efficiency (E_{glob}), and local efficiency (E_{loc}). C_w measures the cliquishness of a typical neighborhood and mirrors the local efficiency of information transfer of the network (Latora and Marchiori, 2001; Watts and Strogatz, 1998). L_w quantifies the ability to propagate parallel information or the global efficiency of a network (Latora and Marchiori, 2001). It reflects the optimal path of information transfer from node i to node j and then economizes the cost of information transfer through the shortest path (Table 2). The global efficiency E_{glob} is similar in purpose to the inverse of the characteristic path length L_w. Nevertheless, E_{glob} is the efficiency of a parallel system, in which all the nodes in the weight network exchange information simultaneously, whereas $1/L_w$ measures the efficiency of a sequential system which exchanges the information node by node (Latora and Marchiori, 2001). Similarly the local efficiency E_{loc} is an average of the local efficiencies and plays a role similar to the clustering coefficient C_w, but only when most of its local subgraphs G are not sparse in a graph, in which C_w is a good approximation of E_{loc} (Table 2).

The small-world properties of a network can be characterized by the normalized clustering coefficient, γ, and the normalized characteristic path length, λ. A real network is considered to be a small-world network if it satisfies the following criteria: $\gamma = C_w^{real}/C_w^{rand} >> 1$ and $\lambda = L_w^{real}/L_w^{rand} \approx 1$ (Humphries and Gurney, 2008; Watts and Strogatz, 1998). Here C_w^{rand} and L_w^{rand} represent the means of corresponding indices derived from the matched random network created using a modified Maslov's wiring program (Maslov and Sneppen, 2002), which preserves the same number of nodes, edges, and degree distribution as the real brain networks obtained from actual subjects.

Regional parameters of the human brain anatomical networks

We used the degree, regional efficiency and betweenness centrality to describe the regional properties of the anatomical networks. The degree (K_i) of a node is the number of connections linking the node. The regional efficiency (*regEff*) is the inverse value of the mean harmonic shortest path length between node i and all other nodes in the network (Achard and Bullmore, 2007). The betweenness centrality (B_i) indicates the number of shortest paths between pairs of other

Table 2
Mathematical definitions of the global and regional parameters used in the current study.

Network properties measures		Definitions	Notes
Global parameters	Cluster coefficient	$C_i = \frac{2}{K_i(K_i-1)} \sum_{j,k} (\tilde{w}_{ij}\tilde{w}_{jk}\tilde{w}_{ki})^{1/3}$	K_i is the degree of node i, and $\tilde{w}_{ij}$ is the weight which is scaled by the largest weight in the network, $\tilde{w}_{ij} = w_{ij}/\max(w_{ij})$
	Characteristic path length	$L_p = \frac{1}{\frac{1}{N(N-1)} \left(\sum_{j \neq i \in G} \frac{1}{L_{ij}} \right)}$	L_{ij} is the shortest path length between node-pair (i,j)
	Global efficiency	$E_{glob}(G) = \frac{1}{N(N-1)} \sum_{i \neq j \in G} \frac{1}{L_{ij}}$	
	Local efficiency	$E_{loc}(G) = \frac{1}{N} \sum_{i \in G} E_{glob}(G_i)$	$E_{glob}(G_i)$ is the global efficiency of G_i, the sub-graph composed of the neighbors of node i
Regional parameters	Degree	$K_i = \sum_{j \neq i} E_{ij}$	E_{ij} is the (i,j)th element of the adjacency matrix
	Regional efficiency	$regEff = \frac{1}{N-1} \sum_{j \neq i \in G} \frac{1}{L_{ij}}$	
	Betweenness centrality	$B_i = \sum_{j \neq i \neq k \in G} \frac{\delta_{jk}(i)}{\delta_{jk}}$	$\delta_{jk}(i)$ is the number of the shortest paths between node j and k that pass through the node i within the graph G

nodes that pass through the node (Linton, 1977). The definitions of all these parameters are listed in Table 2.

Following the methods used in previous studies (Gong et al., 2009a; Yan et al., 2011), we defined the hub regions of the anatomical networks according to the betweenness centrality. To identify the hub regions, we calculated the normalized nodal betweenness, $b_i = B_i / \langle B \rangle$, where $\langle B \rangle$ represents the average betweenness of the network. A node was identified as a hub if it satisfied the criterion $b_i > \text{mean} + \text{std}$, that is that the values of the normalized nodal betweenness had to be one standard deviation greater than the average normalized betweenness of the network.

Reconstruction of the corticospinal tract

The corticospinal tract (CST) contains primarily motor axons that conduct impulses from the brain to the spinal cord. It plays an important role in movement, because half of its fibers arise from the primary motor cortex and the rest from the supplementary motor area, premotor cortex, somatosensory cortex, parietal lobe, and cingulate gyrus. However, the CST did not appear in our constructed anatomical networks because although the primary motor cortex that it connects with is included in the AAL template, the spinal cord or brainstem that it connects with is not. In order to determine the possible effect of intensive gymnastic training on the properties of the CST, we defined the CST between the primary motor cortex and the midbrain using DTIstudio software, which follows the drawing strategy described by Wakana et al. (2007). We defined the first ROI as the entire cerebral peduncle at the level of the decussation of the superior cerebellar peduncle and then selected a bundle of trajectories that reach the primary motor cortex (Fig. 6a). As long as the trajectories to the primary motor cortex are defined, the size of the second ROI can be arbitrary (Wakana et al., 2007). For a given subject, we then calculated the mean fractional anisotropy (FA) for the CST by averaging the FA values of all the voxels that form the three-dimensional tracts derived from tractography. To determine which microstructural properties had changed during training, we also examined the values of the axial diffusivity (AD, $\lambda_\parallel = \lambda_1$) and radial diffusivity (RD, $\lambda_\perp = (\lambda_2 + \lambda_3)/2$) of the CST. These values respectively represent the diffusivity of water molecules in directions that are perpendicular or parallel to the principal axis of diffusion in anisotropic regions of the white matter. Finally, we compared the mean FA, RD and AD of the bilateral CST between the champions and the controls.

Statistical analysis

Again following the method in a previous study (Bai et al., 2012), we used the network-based statistic (NBS) approach to localize specific connected components in which the anatomical connectivity was significantly different between the two subject groups. In brief, we first determined the most consistent connections, that is the backbone network, within each subject group by performing a nonparametric one-tailed sign test ($p < 0.001$, uncorrected) (Gong et al., 2009a). Next, the most consistent connections for each subject in the two groups were detected. Then the NBS approach, in which the *t*-statistic computed for each pairwise association is thresholded to construct a set of suprathreshold links, was conducted within the consistent connections. Any connected components that were present in the set of suprathreshold links and the number of links they were comprised of were thus identified. To estimate the significance of each component, the null distribution of the connected component size was empirically derived using a nonparametric permutation approach (10,000 permutations). Finally, a corrected *p* value for a connected component of size *M* found in the non-randomized data was then determined by finding the proportion of the 10,000 permutations for which the maximal connected component was larger than *M*. For a detailed description of the NBS approach, see the study by Zalesky et al. (2010a).

Between-group differences in the graph-based metrics (global parameters, C_w, L_w, E_{glob}, and E_{loc}; regional parameters, K_i, *regEff* and B_i)

of the anatomical networks were tested by nonparametric permutation tests (Wang et al., 2012; Zhang et al., 2011). Briefly, each subject was randomly assigned to one of two random groups consisting of the same number of subjects as the champion group and control group. This procedure was repeated for 10,000 permutations, resulting in a sampled between-group difference null distribution for each of graph-based metric. Finally, we assigned a *p*-value to the between-group differences by computing the proportion of the differences that exceeded the null distribution values. A significance threshold of $p < 0.05$ was used for testing each of the graph-based metrics. The Bonferroni method was used to correct for multiple comparisons when we tested the statistically significant difference of the regional parameters. Notably, to investigate any potential covariate-related effects, we included age, gender and the age–gender interaction as nuisance covariates throughout the entire analysis (Gong et al., 2009b; Tian et al., 2011; Wang et al., 2012; Yan et al., 2011).

In addition, we performed a Pearson's correlation analysis to detect the relationship between years of training and the global parameters (C_w, L_w, E_{glob}, and E_{loc}) of the world class gymnasts.

Results

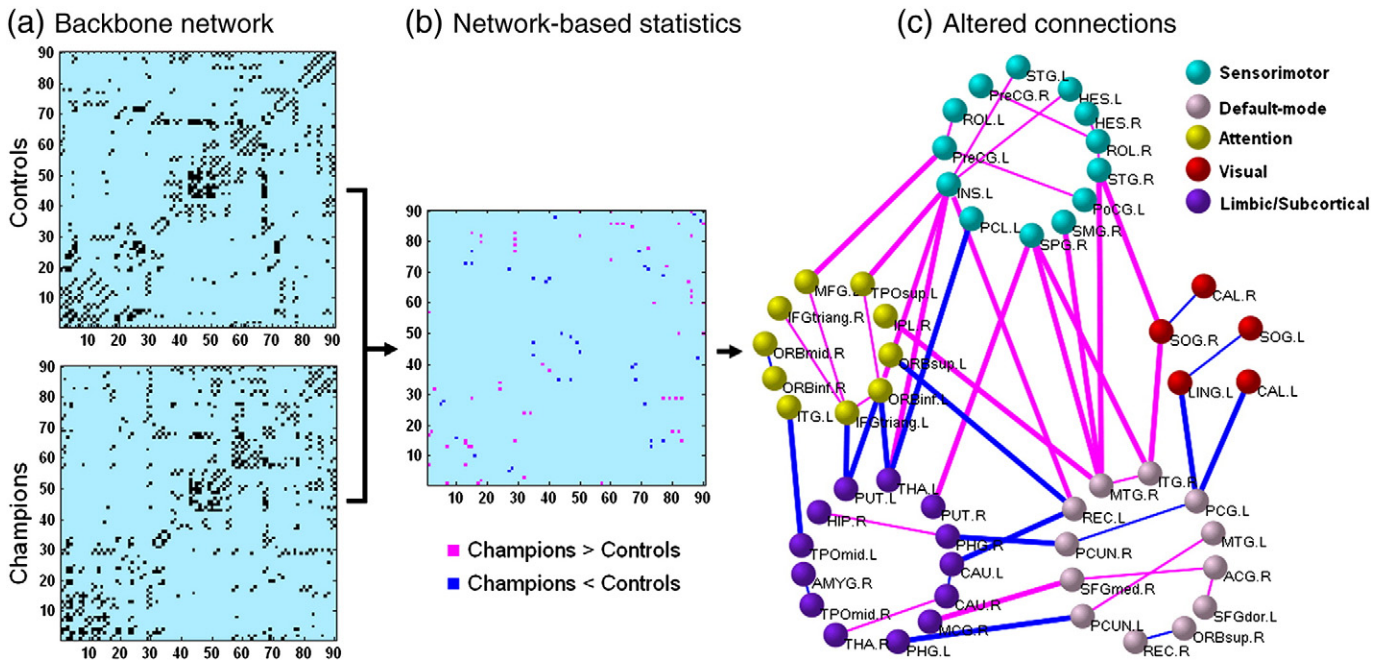*Changes in the connectivity characteristics in the champions*

The NBS was used to identify any connected components in which the anatomical connectivity appears to have been altered by long-term intensive gymnastic training. We localized the connected sub-network (53 nodes and 48 edges) that was significantly different between the two subject groups (Fig. 1). The neural nodes are often categorized into five functional systems — the sensorimotor, default-mode, attentional, visual, and limbic/subcortical systems (He et al., 2009). Out of the altered edges, 30 showed significantly greater connection density (magenta lines in Fig. 1c), whereas 18 edges showed significantly lower connection density (blue lines in Fig. 1c) in the champions than in the controls. Significantly, most of the edges (24/30) with greater connection density that were identified in the champions were linked to regions that were located in the sensorimotor, attentional, and default-mode systems. These 24 edges can be classified into 15 intra-system connections and 9 inter-system connections. Almost all of the increased inter-system connections (8/9) were between the sensorimotor system and the attentional system or between the sensorimotor system and the default-mode system. However, most of the anatomical connections that showed decreased densities in the champions (10/18) were primarily between the limbic/subcortical system and the sensorimotor, attentional or default-mode systems.

Global parameters of the human brain anatomical networks

Statistical comparisons were performed to detect significant differences in the global parameters (C_w, L_w, E_{glob}, and E_{loc}) of the whole brain anatomical networks between the two subject groups. We detected significantly higher values of E_{loc} and E_{glob} but a significantly lower value of L_w in the anatomical networks of the champions compared with the controls. However, we found no statistically significant difference in the value of C_w in the anatomical networks between the two subject groups (Fig. 2 and Inline Supplementary Table S2). We analyzed the correlation between the years of training and the global parameters (C_w, L_w, E_{glob}, and E_{loc}) of the world class gymnasts. Fig. 3 reveals a tendency for the global parameters to change with years of training, but no significant correlation ($p < 0.05$) was detected between years of training and any of these global parameters.

Inline Supplementary Table S2 can be found online at http://dx. doi.org/10.1016/j.neuroimage.2012.10.007.

We tested the small-world properties of the anatomical networks for the champions and the controls and found $\gamma = 3.43 \pm 0.32$ for the champions and $\gamma = 3.88 \pm 0.24$ for the controls, which means that the

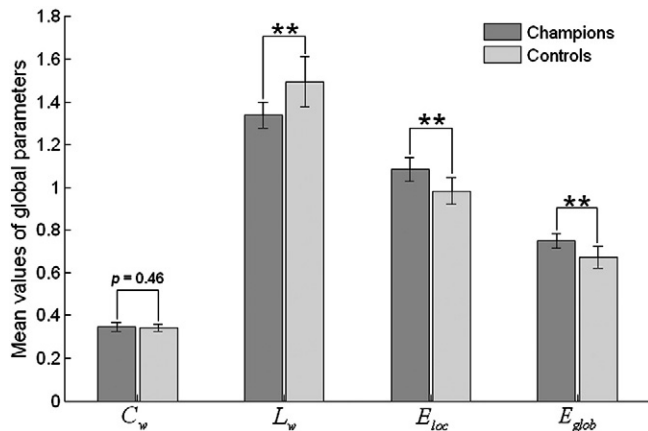## (a) Backbone network   (b) Network-based statistics   (c) Altered connections

Fig. 1. Altered anatomical connections in the world class gymnast group identified using the network-based statistic (NBS) approach. (a) The binarized backbone connections within each group were determined by performing a nonparametric one-tailed sign test. (b) The NBS identified altered connections within the consistent connections as shown by the adjacency matrix. (c) The pairs of brain regions in which the anatomical connections were altered belong to 5 functional systems (sensorimotor, default-mode, attention, visual and limbic/subcortical) which are color-coded as cyan, pink, yellow, red and purple, respectively. Links color-coded in magenta (blue) represent significantly greater (lesser) connection density. The thick (thin) lines represent edges with significant differences in the inter-system (intra-system) connections.
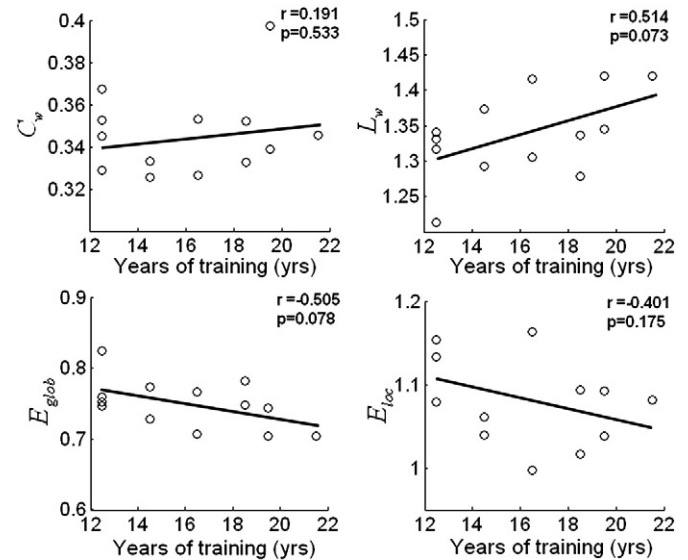
clustering coefficients were approximately 3 times higher than those of a comparable random network for both subject groups. However, we found $\lambda = 1.28 \pm 0.03$ for the champions and $\lambda = 1.28 \pm 0.04$ for the controls. These values near 1 indicated that the path lengths in the two subject groups were approximately equivalent to those of random networks. Our results showed that the anatomical networks corresponding to the two subject groups exhibited small-world properties, a finding which is consistent with previous diffusion tractography studies of human brain anatomical networks (Hagmann et al., 2007, 2008; Iturria-Medina et al., 2008).

Regional parameters of the human brain anatomical networks

Table 3 lists the results of statistical comparisons of the regional parameters (degree K_i, regional efficiency *regEff*, and betweenness centrality B_i) of the anatomical networks between the two subject groups ($p < 0.01$, Bonferroni corrected). We found eight brain regions with significantly higher degrees and ten brain regions with significantly higher regional efficiency in the anatomical networks of the

Fig. 2. Bar plot of statistical comparisons of four global topological parameters of the anatomical networks between the world class gymnasts and the controls. The analysis was repeated with age, gender and age–gender interaction included as nuisance covariates. The symbol (**) denotes that the level of significant difference satisfies $p < 0.01$. (C_w — weighted clustering coefficient, L_w — weighted characteristic shortest path length, E_{loc} — local efficiency, E_{glob} — global efficiency,).

Fig. 3. Tendency of the global parameters (C_w, L_w, E_{glob} and E_{loc}) of the anatomical networks to change with years of training for the world class gymnasts. No significant correlation was detected between the number of years of training and any of these global parameters of the anatomical networks for the champions.

Table 3
Statistical comparison of the regional parameters of the brain anatomical networks between the world class gymnasts and the controls.

Regions	Location	Mean		p-Value	
		K_i	regEff	K_i	regEff
PreCG.L	Primary	21 (12)	0.99 (0.72)	2.00e–4	< 1.0e–4
MFG.L	Association	26 (13)	1.07 (0.73)		1.00e–4
IFGtriang.L	Association	25 (16)	1.03 (0.75)	–	3.00e–4
ORBinf.L	Paralimbic	22 (12)	0.91 (0.63)	–	< 1.0e–4
ACG.R	Paralimbic	16 (5)	0.86 (0.49)	< 1.0e–4	< 1.0e–4
CAL.R	Primary	11 (21)	0.65 (0.80)	< 1.0e–4	–
PoCG.L	Primary	24 (16)	0.99 (0.78)	< 1.0e–4	1.00e–4
HES.R	Primary	7 (1)	0.64 (0.27)	1.00e–4	2.00e–4
STG.R	Association	24 (9)	0.93 (0.59)	< 1.0e–4	<1.0e–4
TPOsup.L	Paralimbic	14 (4)	0.74 (0.40)	< 1.0e–4	1.00e–4
MTG.R	Association	28 (17)	0.96 (0.74)	< 1.0e–4	3.00e–4

Note: the text shaded in gray stands for the regions showing statistically significant differences in degree (K) as well as in regional efficiency (regEff) of the anatomical networks, and the symbol "–" stands for no statistically significant difference between the two subject groups. The group-averaged degree and regional efficiency corresponding to the champions (controls) are presented. The statistical analysis was repeated by including age, gender, and the age–gender interaction as nuisance covariates.

champions compared with the controls. No region exhibited a significant between-group difference in betweenness centrality. Seven of the regions showed significant differences in both degree and regional efficiency, as shown in Fig. 4. The involved brain regions primarily included the left precentral gyrus (PreCG.L), left postcentral gyrus (PoCG.L), right anterior cingulate gyrus (ACG.R), and the temporal lobes [right Heschl gyrus (HES.R), right superior temporal gyrus (STG.R), left temporal pole: superior temporal gyrus (TPOsup.L), right middle temporal gyrus (MTG.R)]. We found no statistically significant difference in betweenness centrality between the anatomical networks of the two subject groups ($p < 0.01$, Bonferroni corrected).

Hub regions in the human brain anatomical networks

Fig. 5a shows a plot of the mean normalized betweenness centrality b_i for the 90 brain regions in descending order for the champions and controls. In each of the two subject groups we identified twelve hub regions, which are listed in Table 4. Although the number of the hubs was identical for the two subject groups, the location of the hubs was not completely the same (Fig. 5b). Several hubs, such as the bilateral insula, the right middle frontal gyrus, and the right hippocampus, were specific to the champions. In order to show the similarities in the spatial patterns of the node betweenness of the two groups, we plotted the coincidence of the normalized betweenness centrality of these hubs in the anatomical networks of the champions and controls ($r = 0.722$) in Fig. 5c. For comparison purposes, we also listed the hubs of the human brain networks identified in previous studies in Table 4.

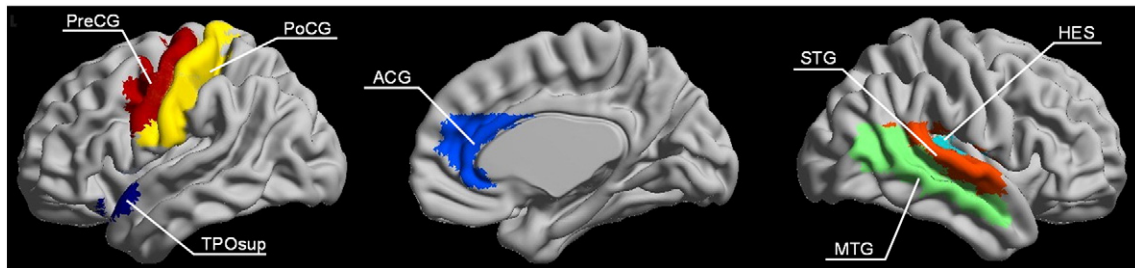*White matter changes in the world class gymnasts*

Figs. 6c and d show the reconstructed bilateral CST for a champion and a control, respectively. We found statistically significantly higher FAs in both the left CST ($p = 0.012$) and the right CST ($p = 0.011$) of the champions compared to the controls (Fig. 6b). Because increases in the FA in white matter can occur due to either a relative decrease in RD or a relative increase in AD or both, we performed a further analysis to examine the group differences in each of these components separately in the CST. Fig. 7 shows decreased RD values in the bilateral CST of the champions as compared to the controls (left: $p = 0.014$, right: $p = 0.030$) but no difference in the AD of the bilateral CST. In addition, we found no significant hemispheric difference in the mean FA, AD or RD for the CST.
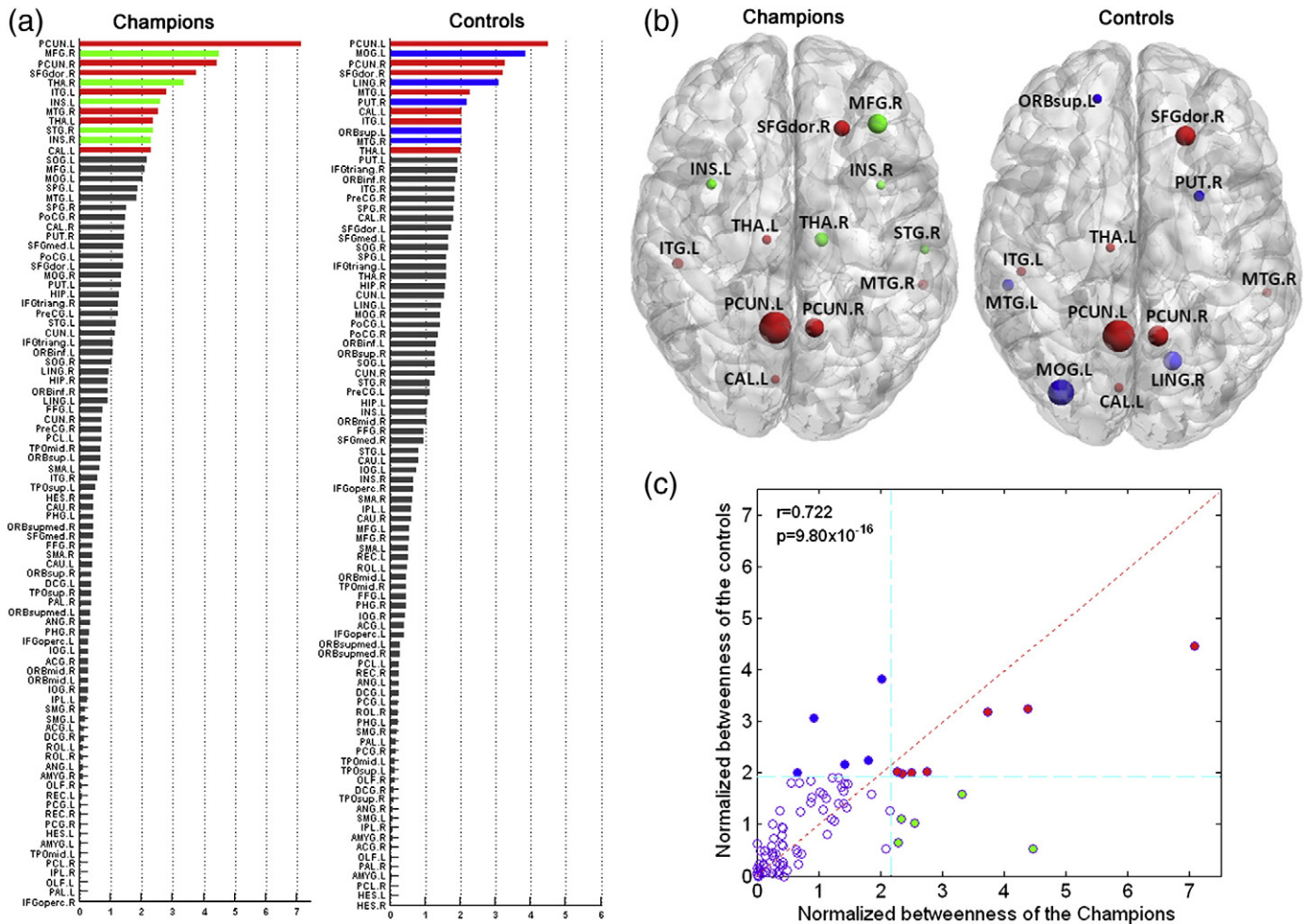
Discussion

In this study, we identified altered connected components, as indicated by between-group differences, that appear to have been induced by long-term intensive motor training, and we compared the topological properties of the human brain anatomical networks of world class gymnasts with those of a control group. Consistent with previous studies, we found that the anatomical networks of both the champions and the controls showed small-worldness. Furthermore, we detected significant differences between the world class gymnasts and the controls in the global and regional properties of the anatomical networks and found changes in the properties of the CST that are likely to have been induced by the champions' long-term intensive gymnastic training or be the result of their innate predisposition or a combination of the two.

Changes in connectivity characteristics in the champions

We found that most of the additional edges (24/30) that were identified in the champions were linked to regions that were located in the sensorimotor, attentional and default-mode systems. The sensorimotor system has been demonstrated to be the central module in the human brain network (He et al., 2009) and plays an important role in behavioral performance (Todorov, 2004). The default-mode system is implicated in the processing of episodic memory (Greicius et al., 2003), and the attention system is predominantly involved in attention processing (Corbetta and Shulman, 2002). These neuroanatomical adaptations that appear to have been formed in response to training suggest that movement, attention and memory all played essential roles in the gymnastic training of the champions. In addition, most of the increased inter-system connections of the sensorimotor system (8/11) were related to the attentional and default-mode systems. This may indicate that the sensorimotor system plays a critical role in coordinating information transfer from the attentional and default-mode systems. Concluding that the world class gymnasts acquired the extraordinary motor

Fig. 4. Rendering plot of the detected brain regions with statistically significant high values of the degree and regional efficiency of the anatomical networks of the world class gymnasts compared with those of the controls. The analysis was repeated with age, gender, and the age–gender interaction included as nuisance covariates. The results are viewed in a sagittal orientation of the bilateral hemispheres. See Table 3 for more details.

Fig. 5. Hub regions detected in the human brain anatomical networks of the world class gymnasts and the controls. (a) Bar plot of the values of mean normalized betweenness centrality b_i for the 90 brain regions in descending order for the champions. (b) Rendering plot of the hub regions of the anatomical networks for the two subject groups. The size of the node represents the magnitude of the normalized betweenness centrality b_i. Nodes color-coded in red represent hub regions detected in the anatomical networks of both the subject groups. Nodes color-coded in green (blue) represent hub regions specific to the champions (controls). The location of the regions was visualized with the Brainnet View software (http://www.nitrc.org/projects/bnv). (c) Correspondence of the normalized betweenness centrality between the anatomical networks of the champions and the controls. Circles are color-coded the same as in (b).

ability needed to control each part of their bodies by coordinating the functions of attention and memory seems reasonable.

Global parameters of the human brain anatomical networks

We found that the anatomical networks of both the subject groups exhibited small-world properties, a finding which is consistent with previous studies (Gong et al., 2009a; Hagmann et al., 2008; Iturria-Medina et al., 2008; Yan et al., 2011). Small-worldness supports both integrated and distributed information processing and maximizes the efficiency of propagating information at a relatively low cost (Bassett and Bullmore, 2006). Although topological parameters are quantitatively unequal across various human brain network studies due to individual differences such as age and gender (Gong et al., 2009b; Yan et al., 2011), identifying small-worldness as a property of the brain network has been common to a number of studies (Bai et al., 2012; Hagmann et al., 2008; Iturria-Medina et al., 2008; Zalesky et al., 2011). Our results also support the concept that small-world topology is a widespread fundamental principle of our efficient brain networks.

Furthermore, we detected significantly greater values of E_{loc} and E_{glob}, but a significantly lower value of L_w in the anatomical networks corresponding to the champions compared with the controls (Fig. 2). Elite athletes are known to be equipped with many advantageous

strategies and processes, including perceptual discrimination, visual search skills (Farrington-Darby and Wilson, 2006), decision making, situation awareness (Starkes and Ericsson, 2003), and explicit knowledge about their particular domain (Renshaw and Fairweather, 2000; Ste-Marie, 1999). The increase in the global parameters E_{loc} and E_{glob} may indicate that the champions can convert more efficiently and quickly between these strategies and processes, thus allowing them to accomplish highly difficult and complex movements.

Regional parameters of the human brain anatomical networks

Our study indicated a significant difference in the regional properties of the anatomical networks between the world class gymnasts and the controls (Table 3 and Fig. 4). We detected a greater degree and higher regional efficiency in the precentral gyrus (PreCG), postcentral gyrus (PoCG), anterior cingulate gyrus (ACG), and the temporal lobes (HES, STG, TPOsup, MTG) in the champions. The functions of these regions are known to be related to motor, sensory control, visual and attention functions. However, none of the regions exhibited a significant between-group difference in betweenness centrality. This may indicate that betweenness centrality is relatively insensitive to differences between the champions and the controls.

Table 4
Hub regions determined in the human brain anatomical networks of the world class gymnasts and the controls.

Hub regions	Location	Champions (b_i)	Controls (b_i)	Identified as a hub in previous studies Anatomical networks	Functional networks
PCUN.L	Association	Y (7.08)	Y (4.47)	1, 2, 4, 5, 6, 8	9, 12, 13
MFG.R	Association	Y (4.46)	N	3, 4	9, 10, 11
PCUN.R	Association	Y (4.38)	Y (3.23)	1, 2, 4, 5, 6, 8	9, 12, 13
SFGdor.R	Association	Y (3.73)	Y (3.18)	1, 2, 3, 5, 8	9, 11
THA.R	Subcortical	Y (3.32)	N	4	12
ITG.L	Association	Y (2.76)	Y (2.02)	1	9, 10, 13
INS.L	Paralimbic	Y (2.56)	N	4, 5, 7, 8	13
MTG.R	Association	Y (2.51)	Y (2.00)	1, 3, 7	9, 10, 13
THA.L	Subcortical	Y (2.35)	Y (1.97)	4, 5	12
STG.R	Association	Y (2.34)	N	6	10, 13
INS.R	Paralimbic	Y (2.28)	N	7, 8	11
CAL.L	Primary	Y (2.27)	Y (2.03)	1	9
MOG.L	Association	N	Y (3.82)	1, 2, 3, 4, 5	9,10 , 11
LING.R	Association	N	Y (3.07)	1	9, 13
MTG.L	Association	N	Y (2.24)	3, 4, 5, 7	9, 10, 13
PUT.R	Subcortical	N	Y (2.17)	4, 5, 8	11
ORBsup.L	Paralimbic	N	Y (2.01)	7	9

1. Yan et al. (2011).
2. Gong et al. (2009a).
3. He et al. (2007).
4. Shu et al. (2009).
5. Li et al. (2009).
6. Hagmann et al. (2008).
7. Bassett et al. (2008).
8. Iturria-Medina et al. (2008).
9. Achard et al. (2006).
10. Tian et al. (2011).
11. He et al. (2009).
12. Tomasi et al. (2011)
13. Liao et al. (2010)

Note: the seven brain regions shaded in gray were shared hubs that were found in the anatomical networks of both groups. "Y" stands for regions identified as hubs, and "N" for regions that were not identified as hubs. For comparison purposes, we also listed the related references in which the regions were identified as hubs in the human brain structural or functional networks.

A striking characteristic of gymnastic champions is their superb motor performance under a variety of environmental conditions. The PreCG has been described as being the primary motor area in humans (Naito et al., 2002; Weinrich and Wise, 1982), making it especially important for gymnastic champions throughout their long-term sports experiences. Several fMRI studies have shown consistent activation of the primary motor cortex during motor imagery (Kim et al., 2008; Porro et al., 2000). In a study of the effect of golf training on gray matter density, Bezzola et al. (2011) showed that the process of golf training increased GM density in the premotor area (PMA) that is involved with movement observation. A previous neuroimaging study also demonstrated that motor tasks such as finger tapping or hand grasping consistently activated the contralateral postcentral gyrus, as well as the PreCG and the PMA (Yousry et al., 1997). Thus, our results in these motor related cortices are consistent with these previous findings.

The ACG is the main neural substrate for focused attention (Osaka et al., 2007) and plays a prominent role in action selection (Rushworth, 2008). Neuropsychological and neuroimaging studies have revealed stronger activations in the ACG during motor imagery of gymnastic movements (Munzert et al., 2008). Kim et al. (2008) compared the activations between world-class archers and controls when they were aiming and found significantly higher activations in the right ACG of world-class archers compared with novices. A morphometrical study also suggested a significant increase in GM density in the ACG induced by a juggle training exercise (Boyke et al., 2008). Gymnasts require highly developed attention to their movements and to the game environment when competing or training. Taking into consideration the

important function of focused attention in the ACG, we suggest that plastic changes in the ACG adapted to experience-related motor learning are vital to gymnasts, especially to world class gymnasts.

The middle and superior temporal gyrus is associated with the representation of complex object features and with advanced cognitive functions, such as verbal memory, information processing, and visual perception (Ojemann et al., 2002; Price, 2000). (Kim et al., 2008) showed that the superior and middle temporal gyri were significantly activated when world-class archers concentrated on the target. In a longitudinal analysis, Draganski et al. (2004) demonstrated a significant bilateral expansion of the gray matter in the middle temporal area of a juggler group. These studies suggest that changes in the superior and middle temporal gyri may contribute to learning and to performing complex visuomotor skills by facilitating the reciprocal transfer of visual and movement perception. In our study, the champions showed a high degree and regional efficiency in the temporal gyrus (Fig. 4). This may indicate that they have a great ability to control their professional movements precisely. Our study provides further evidence for changes in the topological properties of the temporal lobes in the anatomical network of champion athletes.
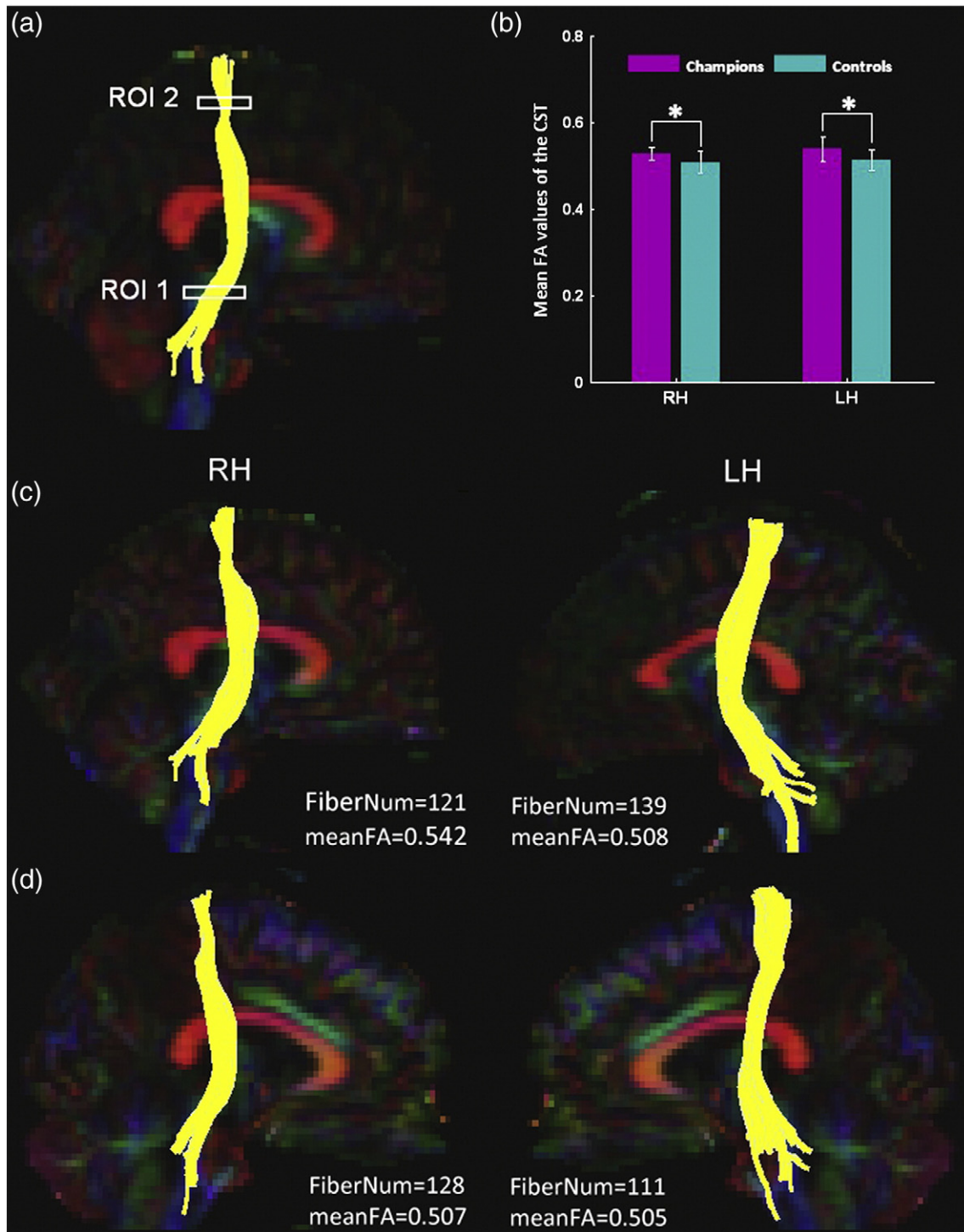
Hub regions in the human brain anatomical networks

Twelve hub regions were identified in the anatomical networks of the two subject groups (Table 4 and Fig. 5). Seven of the champions' hubs and eight of the controls' hubs were located in the association cortices, which receive convergent inputs from other cortical regions (Mesulam, 1998). We found that most of the hubs of the anatomical networks were the same for the two subject groups, a finding which was confirmed by the similarity of the node betweenness derived from the two subject groups (Fig. 5c). Interestingly, the bilateral insula were found as hubs in the champions but not in the controls. In fact, the insula has been identified as a center that ensures heart rate and blood pressure increases at the onset of exercise (Nowak et al., 2005). It is also involved in motor learning (Mutschler et al., 2007) and has been identified as playing an important role in motor recovery from stroke (Weiller et al., 1993). A recent study also showed that the insula plays an important role in sensorimotor integration by strongly coupling with the premotor, sensorimotor, supplementary motor and cingulate cortices (Deen et al., 2011). Although we have no direct evidence that demonstrates that the difference in the insula of the champions is related to a long-term gymnastic training, we find it reasonable to infer that the insula is crucial for gymnasts to coordinate each part of their body through the integration of their somatesthesia with the environment.

White matter changes in the world class gymnasts

The CST is a collection of motor axons that travel between the cerebral cortex of the brain and the spinal cord and is specifically concerned with discrete voluntary skilled movements. We reconstructed the CST that connects the primary motor cortex and the midbrain and detected that the FA value of the bilateral CST of the champions was significantly higher than that of the controls. We further found a decreased RD value in the bilateral CSTs of the champions as compared to the controls. This decrease in RD value indicated that the greater FAs for the bilateral CST of the champions are due to initially lower radial diffusivity in the bilateral CST. Increases in the FA of the bilateral CST results from a change in some microstructural feature (e.g., myelination, packing density, or axon diameter) of white matter that affects radial diffusivity (Song et al., 2005). An increase in myelination will reduce membrane permeability, a change which, in turn, might lead to decreased water molecular diffusive ability in the direction perpendicular to the fiber tracts. Our assumption is that this effect caused the decreased RD and therefore the increased FA in the bilateral CSTs in the champions. Thomas and Gorassini (2005) showed that the intensive treadmill training of muscles affected by spinal cord injury increased the functioning of the
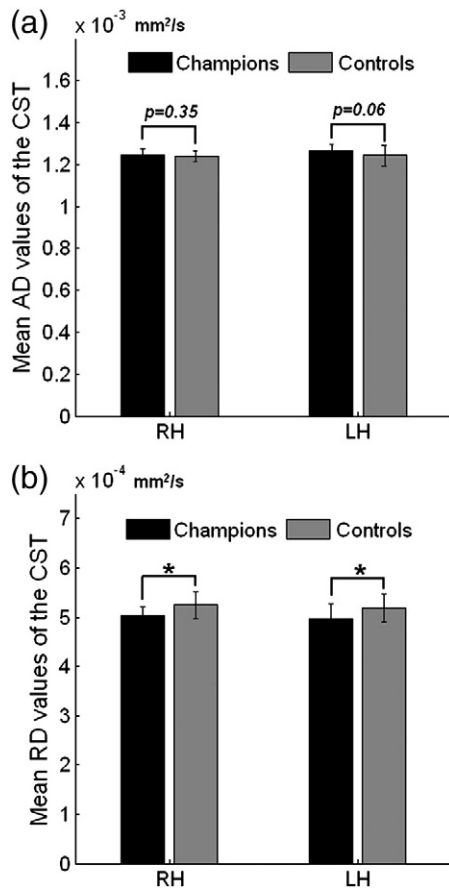
Fig. 6. Diffusion properties of the corticospinal tract (CST) for the world class gymnasts and the controls. (a) Locations of the ROIs selected for building the CST in the sagittal view. (b) Statistical comparison of the value of fractional anisotropy (FA) of the CST between the champions and the controls. The symbol (*) denotes that the level of statistically significant difference satisfies $p < 0.05$. (c) The CST for the first champion who participated in this study in two hemispheres. (d) The CST for the first control subject who participated in this study. RH (LH) — the right (left) hemisphere.

CST. FA has been found to increase in the CST of musicians in response to long-term sensorimotor practice (Bengtsson et al., 2005). Our results may indicate that long-term gymnastic training induces plastic changes in the axonal membrane. This, in turn, might have led to a decrease in the membrane permeability to water, decreasing radial diffusivity and therefore increasing FA in the bilateral CST. Imfeld et al. (2009) also reported decreased FA values in the CST of professional musicians. These mixed findings may have resulted from differences between some of the other studies and this present one in the training subjects and in the motor training regimen.

Further considerations

The present study is limited by several factors. First, the spatial resolution of DTI data (2 mm isotropic) is much larger than the size of axons, so the uncertainty of determining fiber orientation is high

Fig. 7. Diffusivity in the corticospinal tract (CST) of the world class gymnasts and the control group. The champions exhibited significantly high mean axial diffusivity (AD) values in the left CST ($p=0.017$) and low mean radial diffusivity (RD) values in the right CST ($p=0.013$) compared with the controls. *$p<0.05$.

in regions with crossing, twisting or kissing fibers. In addition, the tracking method could influence the accuracy of measures of inter-regional connectivity. We adopted the deterministic tractographic method which is incapable of resolving crossed or twisted fibers (Mori and van Zijl, 2002). This limitation has prompted the development of several different measurement streams including diffusion spectrum imaging (DSI) (Wedeen et al., 2008) and a variety of high angular resolution diffusion imaging (HARDI) methods such as Q-ball imaging and the spherical deconvolution method (Tuch et al., 2002). Although several types of algorithms have been proposed to resolve fibers crossing or kissing or twisting in a voxel, none of these methods are capable of determining the exact origins and terminations of fibers within a cortical area, or of distinguishing efferent/afferent fibers or mixed projections. Second, no definitive answer exists about how to select the network nodes used in constructing human brain anatomical networks. A study has verified that selecting different brain templates to define network nodes influences the topological properties of the brain networks (Zalesky et al., 2010b). Although the AAL template is widely used to define the nodes of brain networks (Iturria-Medina et al., 2008; Yan et al., 2011), many other templates have also been used, including the Brodmann atlas (Vaessen et al., 2010), the ANIMAL (automated nonlinear image matching and anatomical labeling) atlas (He et al., 2008), the LPBA40-atlas (LONI Probabilistic Brain Atlas) (Bassett et al., 2011), the Harvard–Oxford Atlas (Bassett et al., 2011), and the parcellation obtained using Freesurfer (Hagmann et al., 2008). Moreover, more and more researchers have focused on the reproducibility of network analyses derived using high-resolution parcellation (Bassett et al., 2011; Zalesky et al., 2010b). Similarly, no unique definition of

what constitutes an edge in the construction of a human brain anatomical network has been agreed upon. Various studies have defined edges as the number of fibers (Shu et al., 2011), the mean FA values of the connected fibers (Wen et al., 2011), and the weighted fiber density (Hagmann et al., 2007; Hagmann et al., 2008; Yan et al., 2011). Thus, testing the influence of different definitions of node and edge on the topological properties of human brain anatomical networks should be interesting. Third, anatomical networks primarily focus on information processing in the cortical regions of the cerebrum. But the cerebellum is generally accepted as the main region for movement control and is widely associated with the cortex and spinal cord. Networks that contain the cerebellum could be developed in the future in order to explore the plastic effect of long-term gymnastic training on the function and structure of the cerebellum. Fourth, the diffusion gradients (bvecs or B-matrix) introduced by head motion were not rotated when correcting for subject motion in the DTI data from this study (Leemans and Jones, 2009). We think that this effect should be small in comparison with other effects (such as the signal dropout effects or the interaction between motion and field inhomogeneity) that we cannot correct for, and the subjects in this study did not exhibit significant head motion during the DTI acquisition. Another limiting factor is the small sample size, which was necessitated by the small pool of world champion gymnasts available for study. Finally, because we were unable to perform a longitudinal study and because we were limited in our ability to recruit world champions, we cannot completely rule out the possibility that maturation and/or innate predisposition could have caused or contributed to the differences between the champions and the controls.

Conclusion

In summary, we constructed brain anatomical networks for world class gymnasts and controls using DTI and deterministic tractography. Using a network-based statistical analysis approach, we found that the increased connection density primarily occurred in or between the sensorimotor, attentional and default-mode systems in the champion group. Statistical comparisons showed significantly higher values of E_{loc} and E_{glob}, but a significantly lower value of L_w. In addition, several regions that are known to be related to movement showed significantly higher nodal degrees and greater regional efficiency in the anatomical networks corresponding to the champions compared with the controls. We also found that the mean value of the FA of the CST in the champion group was higher than that of the controls. This study provided insights that will allow a better understanding of the differences in brain structure between the world champion gymnasts and non-gymnasts, potentially including brain plasticity in response to long-term intensive gymnastic training. Our results may help to explain gymnastic skill at the highest levels of performance and to understand the neural mechanisms that distinguish expert gymnasts from novices.

Competing interest statement

The authors declare no competing financial interests.

Acknowledgments

Appendix A. Supplementary data

Supplementary data to this article can be found online at http://dx.doi.org/10.1016/j.neuroimage.2012.10.007.

References

Achard, S., Salvador, R., et al., 2006. A resilient, low-frequency, small-world human brain functional network with highly connected association cortical hubs. J. Neurosci. 26 (1), 63–72.

Achard, S., Bullmore, E., 2007. Efficiency and cost of economical brain functional networks. PLoS Comput. Biol. 3, 174–183.

Bai, F., Shu, N., Yuan, Y., Shi, Y., Yu, H., Wu, D., Wang, J., Xia, M., He, Y., Zhang, Z., 2012. Topologically convergent and divergent structural connectivity patterns between patients with remitted geriatric depression and amnestic mild cognitive impairment. J. Neurosci. 32, 4307–4318.

Bassett, D.S., Bullmore, E., 2006. Small-world brain networks. Neuroscientist 12, 512–523.

Bassett, D.S., Bullmore, E., et al., 2008. Hierarchical organization of human cortical networks in health and schizophrenia. J. Neurosci. 28 (37), 9239–9248.

Bassett, D.S., Brown, J.A., Deshpande, V., Carlson, J.M., Grafton, S.T., 2011. Conserved and variable architecture of human white matter connectivity. Neuroimage 54, 1262–1279.

Bengtsson, S.L., Nagy, Z., Skare, S., Forsman, L., Forssberg, H., Ullen, F., 2005. Extensive piano practicing has regionally specific effects on white matter development. Nat. Neurosci. 8, 1148–1150.

Bezzola, L., Merillat, S., Gaser, C., Jancke, L., 2011. Training-induced neural plasticity in golf novices. J. Neurosci. 31, 12444–12448.

Boyke, J., Driemeyer, J., Gaser, C., Buchel, C., May, A., 2008. Training-induced brain structure changes in the elderly. J. Neurosci. 28, 7031–7035.

Bullmore, E., Sporns, O., 2009. Complex brain networks: graph theoretical analysis of structural and functional systems. Nat. Rev. Neurosci. 10, 186–198.

Collignon, A., Maes, F., Delaere, D., Vandermeulen, D., Suetens, P., Marchal, G., 1995. Automated multi-modality image registration based on information theory. Inf. Process. Med. Imaging 3, 263–274.

Corbetta, M., Shulman, G.L., 2002. Control of goal-directed and stimulus-driven attention in the brain. Nat. Rev. Neurosci. 3, 201–215.

Deen, B., Pitskel, N.B., Pelphrey, K.A., 2011. Three systems of insular functional connectivity identified with cluster analysis. Cereb. Cortex 21, 1498–1506.

Draganski, B., Gaser, C., Busch, V., Schuierer, G., Bogdahn, U., May, A., 2004. Neuroplasticity: changes in grey matter induced by training. Nature 427, 311–312.

Farrington-Darby, T., Wilson, J.R., 2006. The nature of expertise: a review. Appl. Ergon. 37, 17–32.

Gong, G.L., He, Y., Concha, L., Lebel, C., Gross, D.W., Evans, A.C., Beaulieu, C., 2009a. Mapping anatomical connectivity patterns of human cerebral cortex using in vivo diffusion tensor imaging tractography. Cereb. Cortex 19, 524–536.

Gong, G.L., Rosa-Neto, P., Carbonell, F., Chen, Z.J., He, Y., Evans, A.C., 2009b. Age- and gender-related differences in the cortical anatomical network. J. Neurosci. 29, 15684–15693.

Greicius, M.D., Krasnow, B., Reiss, A.L., Menon, V., 2003. Functional connectivity in the resting brain: a network analysis of the default mode hypothesis. Proc. Natl. Acad. Sci. U. S. A. 100, 253–258.

Hagmann, P., Kurant, M., Gigandet, X., Thiran, P., Wedeen, V.J., Meuli, R., Thiran, J.P., 2007. Mapping human whole-brain structural networks with diffusion MRI. PLoS One 2, e597.

Hagmann, P., Cammoun, L., Gigandet, X., Meuli, R., Honey, C.J., Wedeen, V.J., Sporns, O., 2008. Mapping the structural core of human cerebral cortex. PLoS Biol. 6, e159.

Hagmann, P., Cammoun, L., Gigandet, X., Gerhard, S., Grant, P.E., Wedeen, V., Meuli, R., Thiran, J.P., Honey, C.J., Sporns, O., 2010. MR connectomics: principles and challenges. J. Neurosci. Methods 194, 34–45.

He, Y., Chen, Z., Evans, A., 2008. Structural insights into aberrant topological patterns of large-scale cortical networks in Alzheimer's disease. J. Neurosci. 28, 4756–4766.

He, Y., Chen, Z.J., et al., 2007. Small-world anatomical networks in the human brain revealed by cortical thickness from MRI. Cereb. Cortex 17 (10), 2407–2419.

He, Y., Wang, J., Wang, L., Chen, Z.J., Yan, C., Yang, H., Tang, H., Zhu, C., Gong, Q., Zang, Y., Evans, A.C., 2009. Uncovering intrinsic modular organization of spontaneous brain activity in humans. PLoS One 4, e5226.

Humphries, M.D., Gurney, K., 2008. Network 'Small-World-Ness': a quantitative method for determining canonical network equivalence. PLoS One 3, e0002051.

Imfeld, A., Oechslin, M.S., Meyer, M., Loenneker, T., Jancke, L., 2009. White matter plasticity in the corticospinal tract of musicians: a diffusion tensor imaging study. Neuroimage 46, 600–607.

Iturria-Medina, Y., Sotero, R.C., Canales-Rodriguez, E.J., Aleman-Gomez, Y., Melie-Garcia, L., 2008. Studying the human brain anatomical network via diffusion-weighted MRI and Graph Theory. Neuroimage 40, 1064–1076.

Jancke, L., Koeneke, S., Hoppe, A., Rominger, C., Hanggi, J., 2009. The architecture of the golfer's brain. PLoS One 4, e4785.

Jiang, H., van Zijl, P.C.M., Kim, J., Pearlson, G.D., Mori, S., 2006. DtiStudio: resource program for diffusion tensor computation and fiber bundle tracking. Comput. Methods Programs Biomed. 81, 106–116.

Keller, T.A., Just, M.A., 2009. Altering cortical connectivity: remediation-induced changes in the white matter of poor readers. Neuron 64, 624–631.

Kim, J., Lee, H.M., Kim, W.J., Park, H.J., Kim, S.W., Moon, D.H., Woo, M., Tennant, L.K., 2008. Neural correlates of pre-performance routines in expert and novice archers. Neurosci. Lett. 445, 236–241.

Latora, V., Marchiori, M., 2001. Efficient behavior of small-world networks. Phys. Rev. Lett. 87, 198701.

Leemans, A., Jones, D.K., 2009. The B-matrix must be rotated when correcting for subject motion in DTI data. Magn. Reson. Med. 61, 1336–1349.

Li, Y., Liu, Y., et al., 2009. Brain anatomical network and intelligence. PLoS Comput. Biol 5 (5), e1000395.

Liao, W., Zhang, Z., et al., 2010. Altered functional connectivity and small-world in mesial temporal lobe epilepsy. PLoS One 5 (1), e8525.

Linton, C.F., 1977. A set of measures of centrality based on betweenness. Sociometry 40, 35–41.

Lo, C.Y., Wang, P.N., Chou, K.H., Wang, J., He, Y., Lin, C.P., 2010. Diffusion tensor tractography reveals abnormal topological organization in structural cortical networks in Alzheimer's disease. J. Neurosci. 30, 16876–16885.

Maslov, S., Sneppen, K., 2002. Specificity and stability in topology of protein networks. Science 296, 910–913.

Mechelli, A., Crinion, J.T., Noppeney, U., O'Doherty, J., Ashburner, J., Frackowiak, R.S., Price, C.J., 2004. Neurolinguistics: structural plasticity in the bilingual brain. Nature 431, 757.

Mesulam, M.M., 1998. From sensation to cognition. Brain 121 (Pt 6), 1013–1052.

Mori, S., van Zijl, P.C., 2002. Fiber tracking: principles and strategies — a technical review. NMR Biomed. 15, 468–480.

Munzert, J., Zentgraf, K., Stark, R., Vaitl, D., 2008. Neural activation in cognitive motor processes: comparing motor imagery and observation of gymnastic movements. Exp. Brain Res. 188, 437–444.

Mutschler, I., Schulze-Bonhage, A., Glauche, V., Demandt, E., Speck, O., Ball, T., 2007. A rapid sound-action association effect in human insular cortex. PLoS One 2, e259.

Naito, E., Roland, P.E., Ehrsson, H.H., 2002. I feel my hand moving: a new role of the primary motor cortex in somatic perception of limb movement. Neuron 36, 979–988.

Nowak, M., Holm, S., Biering-Sørensen, F., Secher, N.H., Friberg, L., 2005. "Central command" and insular activation during attempted foot lifting in paraplegic humans. Hum. Brain Mapp. 25, 259–265.

Oh, J.S., Kubicki, M., Rosenberger, G., Bouix, S., Levitt, J.J., McCarley, R.W., Westin, C.F., Shenton, M.E., 2009. Thalamo-frontal white matter alterations in chronic schizophrenia: a quantitative diffusion tractography study. Hum. Brain Mapp. 30, 3812–3825.

Ojemann, G.A., Schoenfield-McNeill, J., Corina, D.P., 2002. Anatomic subdivisions in human temporal cortical neuronal activity related to recent verbal memory. Nat. Neurosci. 5, 64–71.

Osaka, M., Komori, M., Morishita, M., Osaka, N., 2007. Neural bases of focusing attention in working memory: an fMRI study based on group differences. Cogn. Affect. Behav. Neurosci. 7, 130–139.

Pascual-Leone, A., Amedi, A., Fregni, F., Merabet, L.B., 2005. The plastic human brain cortex. Annu. Rev. Neurosci. 28, 377–401.

Porro, C.A., Cettolo, V., Francescato, M.P., Baraldi, P., 2000. Ipsilateral involvement of primary motor cortex during motor imagery. Eur. J. Neurosci. 12, 3059–3063.

Price, C.J., 2000. The anatomy of language: contributions from functional neuroimaging. J. Anat. 197 (Pt 3), 335–359.

Renshaw, I., Fairweather, M.M., 2000. Cricket bowling deliveries and the discrimination ability of professional and amateur batters. J. Sports Sci. 18, 951–957.

Rushworth, M.F., 2008. Intention, choice, and the medial frontal cortex. Ann. N. Y. Acad. Sci. 1124, 181–207.

Salvador, R., Suckling, J., et al., 2005. Neurophysiological architecture of functional magnetic resonance images of human brain. Cereb. Cortex 15 (9), 1332–1342.

Schmithorst, V.J., Wilke, M., 2002. Differences in white matter architecture between musicians and non-musicians: a diffusion tensor imaging study. Neurosci. Lett. 321, 57–60.

Scholz, J., Klein, M.C., Behrens, T.E., Johansen-Berg, H., 2009. Training induces changes in white-matter architecture. Nat. Neurosci. 12, 1370–1371.

Shu, N., Liu, Y., et al., 2009. Altered anatomical network in early blindness revealed by diffusion tensor tractography. PLoS One 4 (9), e7228.

Shu, N., Liu, Y., Li, K., Duan, Y., Wang, J., Yu, C., Dong, H., Ye, J., He, Y., 2011. Diffusion tensor tractography reveals disrupted topological efficiency in white matter structural networks in multiple sclerosis. Cereb. Cortex 21, 2565–2577.

Song, S.K., Yoshino, J., Le, T.Q., Lin, S.J., Sun, S.W., Cross, A.H., Armstrong, R.C., 2005. Demyelination increases radial diffusivity in corpus callosum of mouse brain. Neuroimage 26, 132–140.

Starkes, J.L., Ericsson, K.A., 2003. Expert Performance in Sports: Advances in Research on Sport Expertise. Human Kinetics, Champaign, IL.

Ste-Marie, D.M., 1999. Expert–novice differences in gymnastic judging: an information-processing perspective. Appl. Cogn. Psychol. 13, 269–281.

Taubert, M., Draganski, B., Anwander, A., Muller, K., Horstmann, A., Villringer, A., Ragert, P., 2010. Dynamic properties of human brain structure: learning-related changes in cortical areas and associated fiber connections. J. Neurosci. 30, 11670–11677.

Thomas, S.L., Gorassini, M.A., 2005. Increases in corticospinal tract function by treadmill training after incomplete spinal cord injury. J. Neurophysiol. 94, 2844–2855.

Tomasi, D., Volkow, N.D., 2011. Functional connectivity hubs in the human brain. Neuroimage 57 (3), 908–917.

Tian, L., Wang, J., Yan, C., He, Y., 2011. Hemisphere- and gender-related differences in small-world brain networks: a resting-state functional MRI study. Neuroimage 54, 191–202.

Todorov, E., 2004. Optimality principles in sensorimotor control. Nat. Neurosci. 7, 907–915.

Tuch, D.S., Reese, T.G., Wiegell, M.R., Makris, N., Belliveau, J.W., Wedeen, V.J., 2002. High angular resolution diffusion imaging reveals intravoxel white matter fiber heterogeneity. Magn. Reson. Med. 48, 577–582.

Tzourio-Mazoyer, N., Landeau, B., Papathanassiou, D., Crivello, F., Etard, O., Delcroix, N., Mazoyer, B., Joliot, M., 2002. Automated anatomical labeling of activations in SPM

using a macroscopic anatomical parcellation of the MNI MRI single-subject brain. Neuroimage 15, 273–289.

Vaessen, M.J., Hofman, P.A.M., Tijssen, H.N., Aldenkamp, A.P., Jansen, J.F.A., Backes, W.H., 2010. The effect and reproducibility of different clinical DTI gradient sets on small world brain connectivity measures. Neuroimage 51, 1106–1116.

Wakana, S., Caprihan, A., Panzenboeck, M.M., Fallon, J.H., Perry, M., Gollub, R.L., Hua, K.G., Zhang, J.Y., Jiang, H.Y., Dubey, P., Blitz, A., van Zijl, P., Mori, S., 2007. Reproducibility of quantitative tractography methods applied to cerebral white matter. Neuroimage 36, 630–644.

Wang, J., Zuo, X., Dai, Z., Xia, M., Zhao, Z., Zhao, X., Jia, J., Han, Y., He, Y., 2012. Disrupted Functional Brain Connectome in Individuals at Risk for Alzheimer's Disease. Biol. Psychiatry. http://dx.doi.org/10.1016/j.biopsych.2012.03.026.

Watts, D.J., Strogatz, S.H., 1998. Collective dynamics of 'small-world' networks. Nature 393, 440–442.

Wedeen, V.J., Wang, R.P., Schmahmann, J.D., Benner, T., Tseng, W.Y.I., Dai, G., Pandya, D.N., Hagmann, P., D'Arceuil, H., de Crespigny, A.J., 2008. Diffusion spectrum magnetic resonance imaging (DSI) tractography of crossing fibers. Neuroimage 41, 1267–1277.

Weiller, C., Ramsay, S.C., Wise, R.J., Friston, K.J., Frackowiak, R.S., 1993. Individual patterns of functional reorganization in the human cerebral cortex after capsular infarction. Ann. Neurol. 33, 181–189.

Weinrich, M., Wise, S.P., 1982. The premotor cortex of the monkey. J. Neurosci. 2, 1329–1345.

Wen, W., Zhu, W., He, Y., Kochan, N.A., Reppermund, S., Slavin, M.J., Brodaty, H., Crawford, J., Xia, A., Sachdev, P., 2011. Discrete neuroanatomical networks are associated with specific cognitive abilities in old age. J. Neurosci. 31, 1204–1212.

Yan, C., Gong, G., Wang, J., Wang, D., Liu, D., Zhu, C., Chen, Z.J., Evans, A., Zang, Y., He, Y., 2011. Sex- and brain size-related small-world structural cortical networks in young adults: a DTI tractography study. Cereb. Cortex 21, 449–458.

Yap, P.T., Fan, Y., Chen, Y., Gilmore, J.H., Lin, W., Shen, D., 2011. Development trends of white matter connectivity in the first years of life. PLoS One 6, e24678.

Yousry, T.A., Schmid, U.D., Alkadhi, H., Schmidt, D., Peraud, A., Buettner, A., Winkler, P., 1997. Localization of the motor hand area to a knob on the precentral gyrus. A new landmark. Brain 120 (Pt 1), 141–157.

Zalesky, A., Fornito, A., Bullmore, E.T., 2010a. Network-based statistic: identifying differences in brain networks. Neuroimage 53, 1197–1207.

Zalesky, A., Fornito, A., Harding, I.H., Cocchi, L., Yucel, M., Pantelis, C., Bullmore, E.T., 2010b. Whole-brain anatomical networks: does the choice of nodes matter? Neuroimage 50, 970–983.

Zalesky, A., Fornito, A., Seal, M.L., Cocchi, L., Westin, C.F., Bullmore, E.T., Egan, G.F., Pantelis, C., 2011. Disrupted axonal fiber connectivity in schizophrenia. Biol. Psychiatry 69, 80–89.

Zhang, Z., Liao, W., Chen, H., Mantini, D., Ding, J.R., Xu, Q., Wang, Z., Yuan, C., Chen, G., Jiao, Q., Lu, G., 2011. Altered functional-structural coupling of large-scale brain networks in idiopathic generalized epilepsy. Brain 134, 2912–2928.